Pb Nano Islands of Magic Heights Formed on the Surface of *i*-$Ag_{42}In_{42}Yb_{16}$ Quasicrystal

By Ana Ribeiro

Department of Physics
University of Liverpool

May 2009

Supervised by Dr. H. R. Sharma

Contents Page

Abstract

The novel structure of *i*-Ag-In-Yb quasicrystals has been put under investigation to analyse its behaviour when high coverages of Pb is deposited on this substrate. This is the first non Al based quasicrystal that has been examined under Ultra-High Vacuum (UHV) conditions. Scanning Tunnelling Microscopy (STM) was used to analyse the islands formed from Pb atoms. Islands of selective heights: 4.3, 5.5 and 6.5 ML showed strong evidence of quantum size effects that occur due to electron confinement.

Introduction

Quasicrystals have only recently been discovered and since then much scientific research has been conducted. The majority of quasicrystals studied have been based on Al composition but only several years ago that an Ag based quasicrystals has been grown into a single grain of millimetre dimensions [1].

The particular quasicrystal being studied in this report (*i*-Ag-In-Yb) is of interest because apart from being the first quasicrystal sample to have been grown as a single-grain and that is not Al-based it also is suitable for UHV conditions. The majority of quasicrystals that have been used in investigations and that are suitable for Ultra-High Vacuum (UHV) conditions were mainly Al-based. Other quasicrystals such as *i*-RE-Mg-Zn and *i*-Cd-Yb were able to grow into single grains and in large size but were unsuitable for UHV experiments due to the fact that Zn and Cd have high vapour pressures so they would evaporate when the vacuum is heated causing contamination in the chamber [2].

Surface studies of quasicrystals have become a rich research topic. Since its discovery much exploration has been done to understand its structural phenomenon. Investigations were done to answer fundamental question such as does the surface relax or reconstructs, are there evidence of step-terrace formations, does the bulk and the surface maintain the same features? Understanding quasicrystals is still at an early stage but so far a great deal of progress has been done. In addition, these new materials show certain interesting properties such as low friction, firmness [3], and non-stickiness.

The project being carried out is a continuation of the outcome and interests in pursuing an understanding on the results arrived in the past experiments. Atomic overlayers of a number of elements were deposited on different quasicrystals with the main aim of obtaining pseudomorphic quasicrystalline thin films of single elements. Only certain elements yield films of quasiperiodic structure. These studies have been limited to Al-based alloys.

This discovery of Ag-based quasicrystal has provided great advantage in expanding on the understanding of the overlayer growth phenomena. It was found that the five-fold surface of the icosahedral Ag-In-Yb quasicrystal showed to be a good template for the atomic overlayer of Pb[1] to form quasicrystalline structures. This system also showed that a second layer of this element can be grown possessing the same quasicrystalline structure [4].

In this project, growth of Pb films at coverages beyond 2 ML was studied. The data obtained for the Pb films was done using STM and the island heights analysed with WSxM programme. It was found that the islands selected specific heights throughout the experiment. The most frequent heights observed were the 1.2 nm, 1.5 nm and 1.8 nm islands.

These islands show evidence of “Magic Heights” which arise from Quantum Size Effects (QSE). This is a result of electron confinement in a potential well. The discrete electronic states or Quantum Well States (QWS) have specific energy values and the states well below the Fermi Level are the states that give rise to the most stable islands [5].

---

[1] Pb was chosen because it has a low surface free energy and thus the elements are more likely to wet the surface.

Chapter 1

Background Information

1.1 Periodic and Quasi-periodic Structures

In crystallography a periodic crystal is assumed to have perfect geometrical points called lattices [6]. Each point is identical to the other and thus translational symmetry can be observed in the crystal lattice.

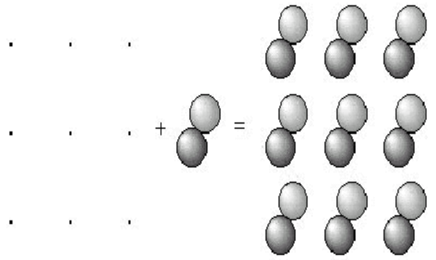

Figure 1 Image showing: Space lattice + basis = Crystal [7].

The space lattice is a lattice of points and the basis represents the group of atoms in each lattice point. The atomic positions in a space lattice are related to the position vector, which is expressed in the form

$$r = \mathbf{a}n_1 + \mathbf{b}n_2 + \mathbf{c}n_3 \tag{1}$$

where **a**, **b** and **c** are unit vectors of the translational symmetry and n_1, n_2 and n_3 are integers. There are 14 particular ways of organising the lattice points in a 3-Dimentional space. The 14 ways of grouping are called the **Bravais Lattices**. Each unit volume associated with the lattice is known as the primitive cell (for a single lattice point) or the unit cell (spatial arrangement of atoms in a cube that displays the full symmetry of the crystal). **Symmetry elements** such as rotations and reflections are present in a crystal structure. These are called **point group** symmetries and consist of 230 different patterns.

It wasn't until 1982 that the idea of non-periodicity (or aperiodicity) but long range order structures could exits. This was a very controversy in the world of crystallography but Dan

Shechtman with other three scientists found that the metal solid of Al-Mn had long range order but with icosahedral symmetry. It also had very sharp diffraction spots but did not indexed to any of the know Bravais lattice [8].

In crystallography there are certain rotational symmetries of order n that are allowed and others that are forbidden. A rotational symmetry of order n or also commonly known as n-fold rotational symmetry describes the rotation of an object by an angle of 360°/n and in which this rotation does not change the object. For example, an object with 2-fold symmetry can have 180° rotation and it would tile perfectly with no gaps. Therefore, symmetries such as 2-, 3-, 4-, and 6-fold are permitted and 5-, 7-, and 10-fold are forbidden.

Structures with these forbidden symmetries became known as quasicrystals, which is short for quasi-periodic crystals.

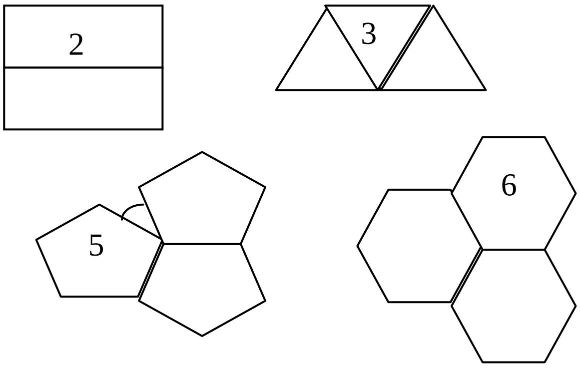

Figure 2 Image showing some of the permitted and forbidden symmetries [9].

Most quasicrystals obey the rules of a three-dimensional **Penrose Tiling**. The Penrose tiling was proposed by Roger Penrose, a Mathematician in Oxford University, who suggested around 1970, that there are possible ways of tiling a structure that is not periodic by just using a few other forms of tiles (or shapes). He was able to cover an aperiodic plane that would exhibit 5- and 10-fold symmetry without leaving any gaps. **Figure 3** is a famously known Penrose tiling that demonstrates another interesting phenomenon in nature. By adding the interior angles of the two rhombic shapes: 72° with 108° and 36° with 144° and then finding the ratio of the areas it results in a value known as the **Golden Ratio**, τ. The Golden Ratio was a number that first appeared in geometric shapes and were a result of taking the ratios of two distances. This value is approximately to 1.6 and is now believed to appear almost everywhere when taking the ratio of two distances, even in the human body.

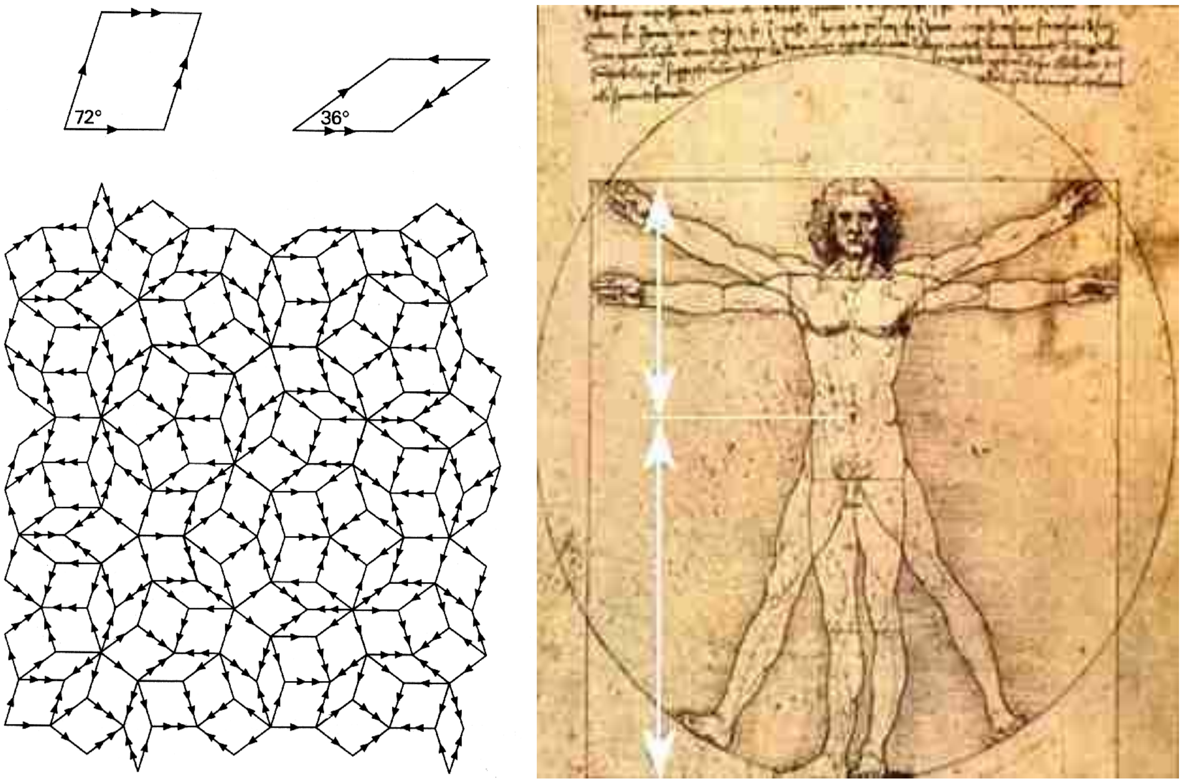

Figure 3 First image illustrates a Penrose tiling with rhombic tiles [9] and the Second image displays the notion that if you take the ratio between the navel and foot to head and navel you are able to find the Golden Ratio [10].

Another procedure of obtaining aperiodic structures but with long range order is by carrying out the **Fibonacci Sequence**. This one-dimensional sequence can be built by setting define rules. If the letter L is the starting point and follows the rule that L→ LS and S→L then a beautifully ordered and non periodic sequence can form. Not all starting points are allowed and the following value is the sum of the previous [6]:

L
LS
LSL
LSLLS
LSLLSLSL
LSLLSLSLLSLLS
...
...
...
etc

The Fibonacci Sequence, the Golden Ratio and the Penrose Tiling are examples of mathematical phenomenon that can be present in quasicrystals.

1.2 Icosahedral Structures

The Icosahedral, *i* quasicrystal is a complex geometric structure that has 31 high symmetry axes of which ten are 3-fold axes, six are 5-fold axes and fifteen are 2-fold axes.

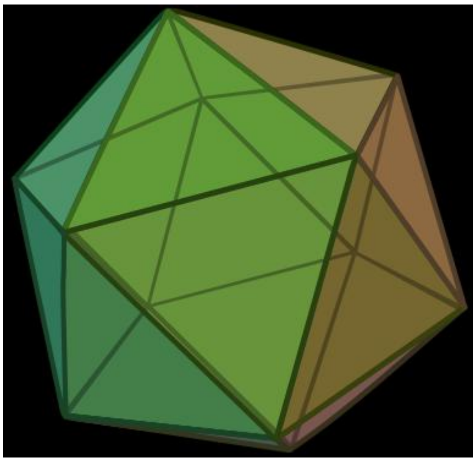

Figure 4 Figure showing an icosahedral shape, which has equilateral triangles as faces [11].

The quasicrystal used in this experiment shows evidence of the fivefold surface.

1.3 Surface Studies

Studying the surfaces of solids is an important process for scientific and technological understanding. The bulk of a solid differs greatly to its surface. When studying the bulk of a solid it is only possible to gather information about the number and types of atoms present in it and their arrangement in space in relation to each other.

However, examining the surface of a solid gives much detailed information about the material under observation. The information obtained at the surface includes chemical compositions, atomic arrangements at the surface, mechanical and electronic properties [12].

Surface atoms have less neighbouring atoms compared to the bulk material. These atoms have “dangling bonds”, which causes the energy to increase. The difference in energy between surface and bulk is referred to as surface free energy. To reduce these “dangling bonds” the surface can rearrange itself to reach a new equilibrium. Two ways that the surface reduce these “dangling bonds” is by 1) the atoms arrange themselves with the surface or undergo *Surface Reconstruction* and 2) the atoms loosen vertically or commonly known as *Surface Relaxation*.

1.4 Growth of Atomic Overlayers

Atomic overlayers are also commonly known as *thin films*. These occur when the deposition of a certain adsorbate covers more than a monolayer on the substrate. The growth of a single-crystal layer on a substrate is denoted as epitaxy. This type of growth can be further divided into two other forms:

- Homoepitaxy - the substance content of film and substrate is the same
- Heteroepitaxy – the substance content of film and substrate is different

The tendency of the film growth is determined by the effects of thermodynamics and non-equilibrium kinetics processes, which leads to three main growth modes [13]:

- Layer-by-layer (Frank-van der Merve)
- Islands (Vollmer-Weber)
- Layer-plus-island (Stranski-Kranstanov)

1.4.1 Growth Modes

The growth modes stated above are described here in detail. The names of each mode were appointed after their investigators:

Frank-van der Merve (FM) – deposited atoms are bound firmly with the substrate and weakly with each other. This affects the growth of the following layer because it requires that the previous layer is completed before the next one starts.

Volmer-Weber(VW) – deposited atoms are firmly bound to each other than to the substrate. This results in the nucleation of islands directly on the surface of the substrate.

Stranski-Kranstanov(SK) – this growth mode behaves in similar ways to the two above. Firstly, the formation of a complete layer (or layers) occurs. Then, the growth of islands happens. This intermediate step, also known as, the Stranski-Kranstanov layer is determined by the nature of each particular material.

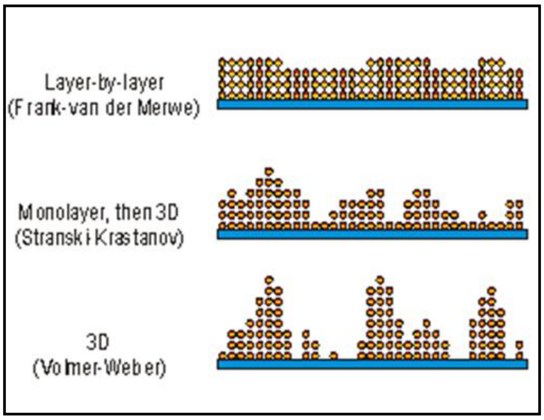

Figure 5 Image illustrating the different growth modes [14].

The manifestation of these growth modes can be further explained by the thermodynamic tendency of the system. Each growth mode can be understood in terms of the surface tension, γ (or interface tension). Surface tension occurs when a system tries to minimise its total surface free energy by reducing its surface area. The contact angle between the surface energies of the substrate and adsorbate are related with the following equation [13]:

$$\gamma_S = \gamma_{S/F} + \gamma_F \cos\varphi \qquad (2)$$

γ_S represents the surface tension of the substrate surface,

$\gamma_{S/F}$ represents the surface tension of the film/substrate interface,

γ_F represents the surface tension of the film surface

cosφ represents the contact angle between the substrate and adsorbate.

For the three cases of growth mode described above, **Equation 2** modifies depending on their conditions:

FM growth mode (layer-by-layer), φ = 0, thus

$$\gamma_S \geq \gamma_{S/F} + \gamma_F \tag{3}$$

VW growth mode (island growth), φ > 0, thus

$$\gamma_S < \gamma_{S/F} + \gamma_F \tag{4}$$

SK growth mode (layer-plus-island): in this case, the growth beginnings with condition from **Equation 3** and then follows condition from **Equation 4**.

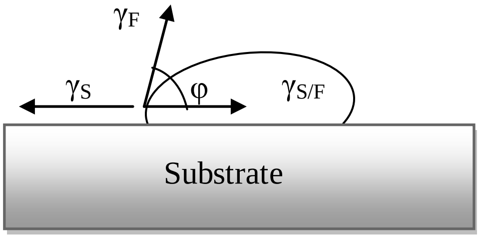

Figure6 Schematic diagram showing an island on a substrate. Arrows show the direction of each surface tention [13].

1.4.2 Growth of Islands

Islands are formed after certain elementary processes take place. The atoms landing on the substrate are travelling at a rate, R and become adatoms with a binding energy, E_{ads}. The adatoms are able to travel within the surface with a diffusion coefficient, D

$$D = \left(\frac{\nu}{4n_0}\right) e^{\left(\frac{-E_{diff}}{k_B T}\right)} \tag{5}$$

where n_0 is the number of site per unit area, k_B is the Boltzmann constant, T is the temperature and E_{diff} is the diffusion activation energy [13].

Figure 7 displays the possible processes that can occur to an atom as it reaches the substrate. The points below describe these possible processes:

- The adatom can re-evaporate if the surface temperature is high enough for this to take place;
- The arriving adatoms can join with the existing clusters or stick onto defect sites, e.g. steps on the substrate;
- Individual adatoms can bond together to create a cluster.

The majority of small clusters diffuse back into single atoms but when clusters grow to a certain size this overcomes the probability of diffusion and it becomes more stable. This arises when the cluster as reach a minimal size by the addition of just one extra atom, also known as the *critical island size i*.

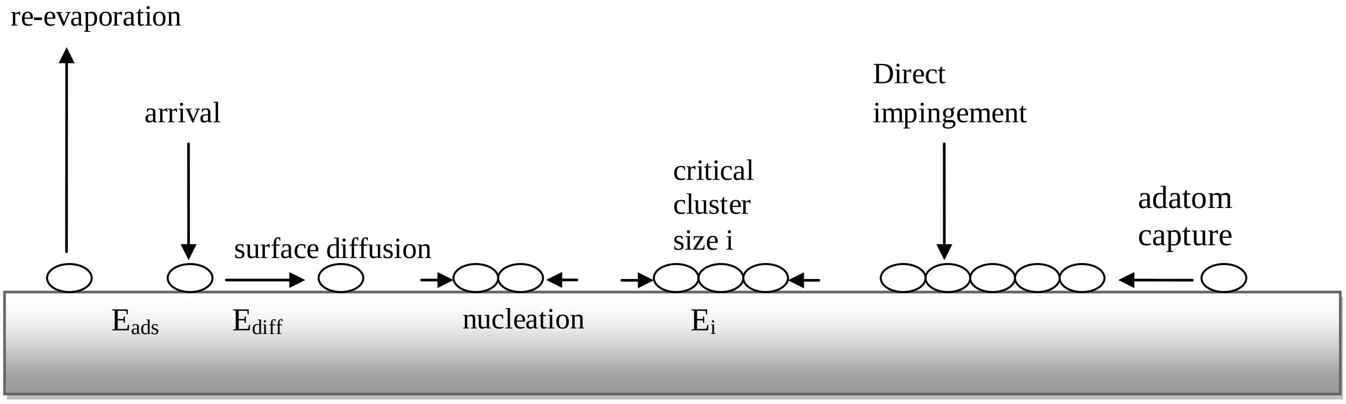

Figure 7 Diagram illustrating some of the elementary processes involved in the growth of islands on surfaces [13].

1.5 Magic Heights

This concept of magic heights can be explained by the simple understanding of the quantum mechanical notion of a “particle in a box”. This basic idea of a “one-dimensional potential well” helps understand the principle of magic heights. Magic Heights are observed as a result of Quantum Size Effect (QSE), which arises from electron confinement [5]. Electrons in a potential well are usually confined and when confinement occurs, discrete states are formed. These discrete states are usually called *Quantum Well States* (QWS). The permitted wave vector, k, for these states is determined by the equation below

$$k = \frac{n\pi}{d} \tag{6}$$

where n is an integer and d is the film thickness. The corresponding energy levels is given by

$$E = \frac{\hbar^2 k^2}{2m} = \frac{\hbar^2}{2m}\left(\frac{n\pi}{d}\right)^2 \tag{7}$$

where m is the mass of the free electron and $\hbar$ is Planck’s constant.

When a thin film layer is deposited on a substrate it acts as a “one-dimensional potential well”, where the motion of electron is perpendicular to the film surface. The energies and widths of quantum well states in a film depend on the film thickness, the dynamics of electron motion in the film, and the confinement potential [15].

Moreover, the band gap observed in materials such as in semiconductors play a fundamental role in quantum well effects. For semiconductors in particularly, the band gap does not allow the electrons to propagate and thus confining the carrier particles.

In the case for metals there are no gaps at the Fermi Level, which give the impression that confinement would not be possible to occur. However, band gaps do happen in metals mainly at the interfaces of substrate/films. Confinement of an electron arises if the energy of the electron is at the band gap of the substrate. In addition, the electronic bands have different directions, which cause gaps around the Fermi Level. This results in a well defined symmetry of band states around the Fermi Level that have. This symmetry is also known as the *symmetry gap* and is relative to other states with different symmetry.

Therefore, even in metals there is a band gap around the Fermi Level but only of a few eV. When a thin-film is deposited on a substrate the electron travels towards the surface and if its energy is within the bulk gap it reflects the electron because it is unable to bond with the bulk states.

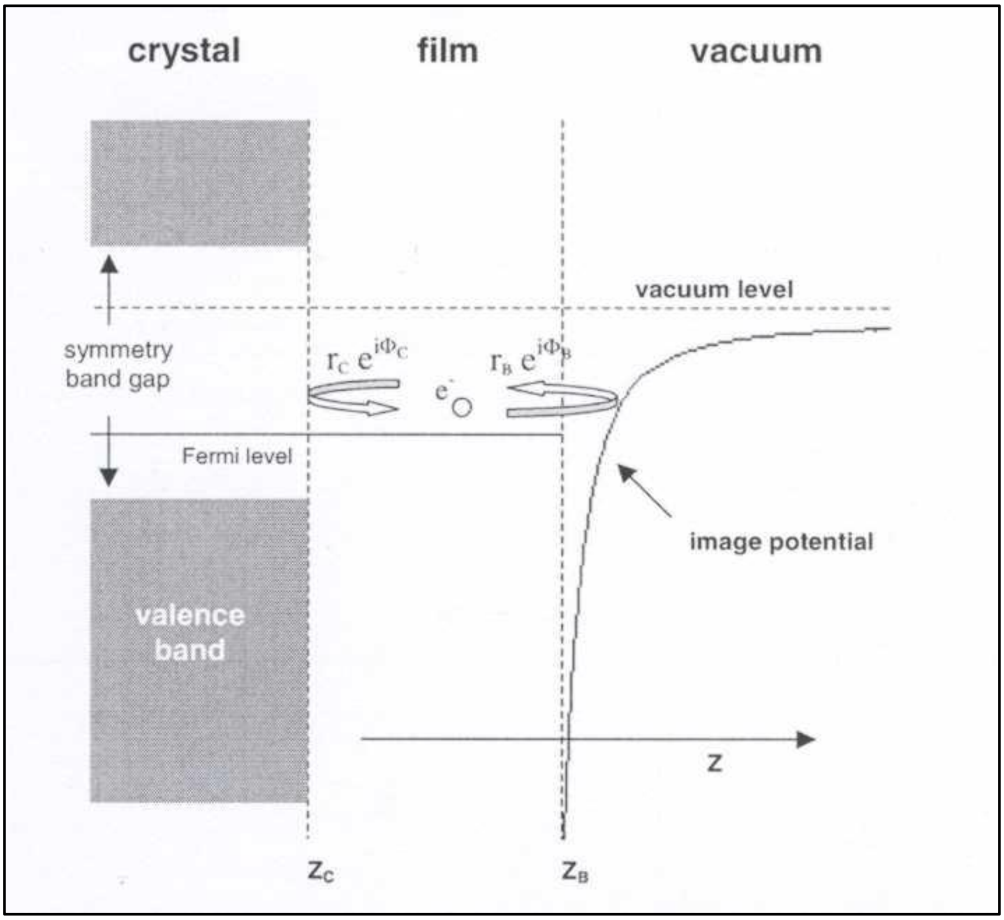

Figure 8 Illustration of the electron being reflected back as it reaches the substrate [16].

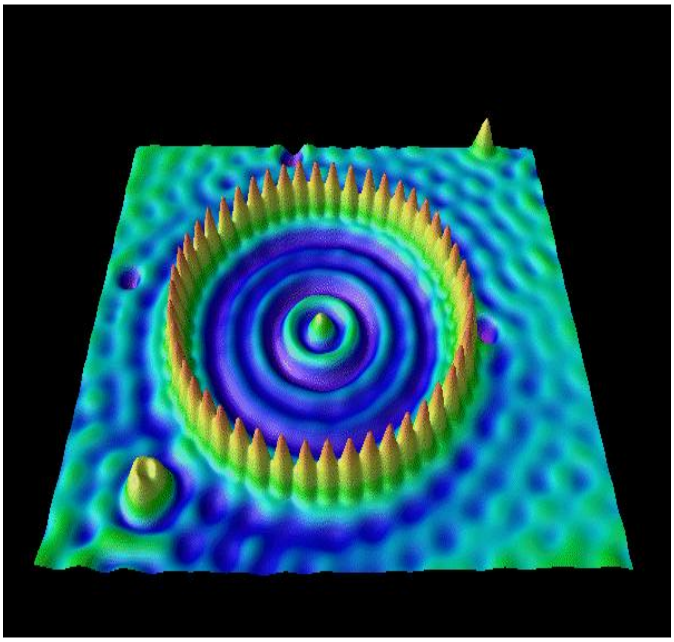

Figure 9 This 71Å diameter "Quantum Corral" illustrates the standing-waves formed by electron confinement [17].

To make **Figure 9**, 48 iron atoms (shown as yellow peaks) were placed in a circle on a copper surface. The "elevation" at each point inside the circle indicates the electron density within the circle. The standing-wave pattern is very similar to the probability distribution function for a particle in a one-dimensional finite potential well. This image was made with a scanning tunnelling microscopy.

Chapter 2

Experimental Procedure and Results

This chapter concentrates on the explanation of sample and apparatus treatment, the technique used, and how the experiment was conducted.

2.1 Ultra-High Vacuum (UHV)

Conducting surface science experiments under UHV conditions is very important to minimise the unknowns so that when probing the surface of the sample one knows that the information being gathered is not being highly affected by other impurities.

The chambers that compose the vacuum are made of special materials. Usually the material is Stainless Steel as this has a low rate of outgassing and provides shielding from magnetic fields.

The pressure obtain by UHV are in the order of 10^{-12} mbars. Such low pressure permits that molecules travelling inside the vacuum can travel for longer distances and with fewer interactions.

An important consideration for vacuum technology is the *mean free path* of a molecule. This determines the average distance that a particle travels in the gas phase between collisions [18].

Another necessity for carrying surface science experiments is that the sample surface is maintained clean. The *sticking coefficient, S* of the gas environment (or impurities) determines the amount of molecules adsorbed on the substrate. Its value can range from 0 to 1, where 0 signifies that there is no adsorption and 1 means that there is complete adsorption. This value is can be affected by other factors such as the temperature, the structure of the substrate, and the amount of coverage.

At much lower pressures the sticking coefficient reduces greatly which allows enough time for experiments to be conducted without a high rate of deposition of impure molecules on the substrate.

To reduce to Ultra-High pressures, a combination of different pumps can be used. Initial, a rotary vane pump is used to reduce the pressure to around 10^{-3}. This pump has a rotor with a vane that is placed off centre. Firstly, the volume expands inside the pump chamber but with continuous rotation the volume compresses until its required pressure is reached. Subsequently, a turbomolecular pump is put into action and this reduces the pressure to a further 10^{-11} mbars with the help of its angled blades that rotate at a speed of approximately 15,000 to 30,000 rpm.

Below is a table showing the different scales for each type of vacuum:

Degree of Vacuum	Pressure, P (mbars[2])
Atmospheric	10^{3}
Low (rough)	1
Medium	10^{-3}
High	10^{-6}
Ultra-High (UHV)	10^{-10}

Table 1 Table shows the values of pressure for the different types of vacuums. These values are approximate values.

During analysis of surfaces using techniques such as STM one requires a low vibration environment. This can be obtained by using an Ion Pump. An Ion Pump ionizes the surrounding gas and with the presence of an electric field it is able to accelerate these ions to an electrode. A magnetic field maintains this ionization process and keeps the ions in the electrode. This effectively removes the ions from the vacuum chamber and provides the inside environment with a reduce amount of particles that collide during the substrate scanning.

---

[2] 1 Torr = 1.33 mbar and 1 atm = 760 Torr = 10^{3} mbar (These are approximate values).

Following insertion of the sample into the vacuum, the entire chamber was *baked out* (this procedure involves heating the chamber to around 430 K for approximately 15 hours to remove any water from the walls). Subsequently the all filaments were required to be degassed. This usually begins by degassing some parts of the apparatus at around 10^{-7} mbars and has the pressure approaches 10^{-9} mbars the more sensitive parts are degassed. This is done so that the filaments do not sublime.

2.2 Surface Preparation

Polishing the surface of the quasicrystal before going through its thorough cleaning in the vacuum chamber increases the production of quality terraces. The quasicrystal surface was polished on a 6 μm, 1 μm and ¼ μm diamond paste. Each paste was used respectively to refine the smoothness of the sample surface. Methanol was utilised at all time to clean the sample and non abrasive absorbent paper for drying it. The quasicrystal was welded onto a sample holder and left in an ultra sonic-bath to remove any extra impurities.

For further cleaning of the surface, argon ions were sputtered with energy of around 3 keV and at room temperature. The ion bombardment removes most of the impurities. Thereafter, annealing takes place at approximately 710 K to remove the embedded Ar atoms and to restore the surface crystallography. This is done for several hours and at pressures that are below 10^{-9} mbars but reaching 10^{-10} mbars. It was found that doing cycles of ion bombardment/annealing also produced a well-ordered atomically clean surface. After cooling the sample it was ready for study. Afterwards, the sample was placed inside the VT-STM[3] vacuum chamber for further preparation.

2.3 Scanning Tunnelling Microscopy (STM)

Scanning Tunnelling Microscopy (STM) is a technique where its operation relies on the quantum mechanical tunnelling of electrons across a small gap (around 1 nm) between an atomically sharp tip and the sample's substrate [14].

The STM images are a two-dimensional plot of the charge density of the surface and not the actually nuclear position. The tunnelling current, j, flows through the vacuum gap with the following relationship:

---

[3] VT-STM stands for Variable Temperature - Scanning Tunnelling Microscopy.

$$j = Ae^{-\text{Ø}d} \tag{8}$$

where Ø is the barrier height, d is the separation between tip and sample and A is a constant. The resolution of the images depend greatly on the current, j and the separation, d. Changing the separation, d by about 1Å can cause changes in the order-of-magnitudes in the current. The electron is allowed to tunnel if it has sufficient energy to overcome the potential barrier but the probability of finding it outside the barrier decreases exponentially.

The scanning of the surface with the tip is controlled by a piezo-electric drive. These are made from piezo-ceramic materials that can produce an electric potential due to an applied mechanical stress. Piezo-electric drives can manoeuvre the tip and maintain the distance between tip-sample to a high precision.

There are two modes in which the STM can be used:

a) Constant current mode – this mode has a feedback loop that keeps a tip-sample current constant as the tip scans over the surface. The separation, d, is therefore maintained constant and the motion in the z-direction (up and down directions) is controlled from the voltage supplied, which provides the mapping information of the surface.

b) Constant height mode – in this operation a feedback loop is used so that the height above the surface is kept constant throughout the scan, i.e. the voltage in the z-direction is constant while the current provided maps the surface. The disadvantage of this mode is that the tip can crash into certain elevations on the sample.

The quality of the tip is very important to build the outline of the charge density of the surface, which will be mentioned in the next section (In addition, suitable voltages are needed for image construction).

STM Tip

The tip used for this experiment was made from Tungsten, W wire. A small piece of wire (about 2-3cm) was suspended and dipped into Potassium Hydroxide (KOH). The drop of KOH was put in a small hole where the liquid hanged from it due to surface tension. A bias of 10V was supplied across the wire and the KOH. It was then placed in its sample holder. The other end of the wire was also etched. Before placing the tip in the chamber, it was placed under a microscope of about 200x optical resolution to see if the tip had a sharp end. Once satisfied with its sharpness the tip is rinsed with methanol and put inside the UHV chamber. For further cleaning the tip was sputtered with Ar^+ ions to remove any oxides. Thereafter, the tip is supposedly clean and ready for use.

To build well resolved images it is necessary that the tip is atomically sharp. However, tips can become asymmetric or have multiple tips that generate blurred images. Occasionally there are chances of picking up impurities or adsorbate molecules with the tip and this is scanned over the surface giving lines across the image instead of the usual charge density images. In such case, the impurities can be removed by nanostructuring the tip. This is done by applying high voltage impulses. Such technique is known for improving the sharpness of the tip.

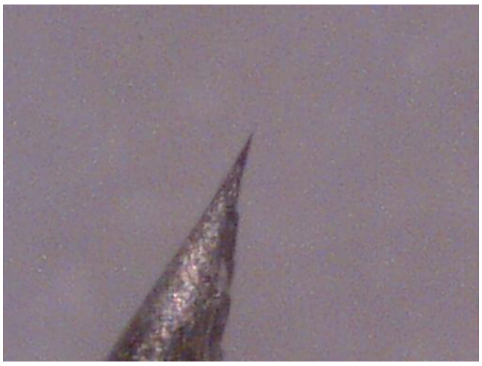

Figure 10 A picture taken from an optical microscope showing a typical sharp tip used for STM [19].

STM Surroundings

The operation of STM is very sensitive to external vibrations. This could affect the quality of the images produced. There are several ways of reducing external vibrations. The STM is usually mounted on a vibration absorber to reduce the noise that arises from the laboratory floor. The STM (or the entire vacuum system) can be placed in a soundproof or quiet room to help reduce vibrations. Inside the vacuum system there are current damping and anti-vibration suspensions to help reduce further noise.

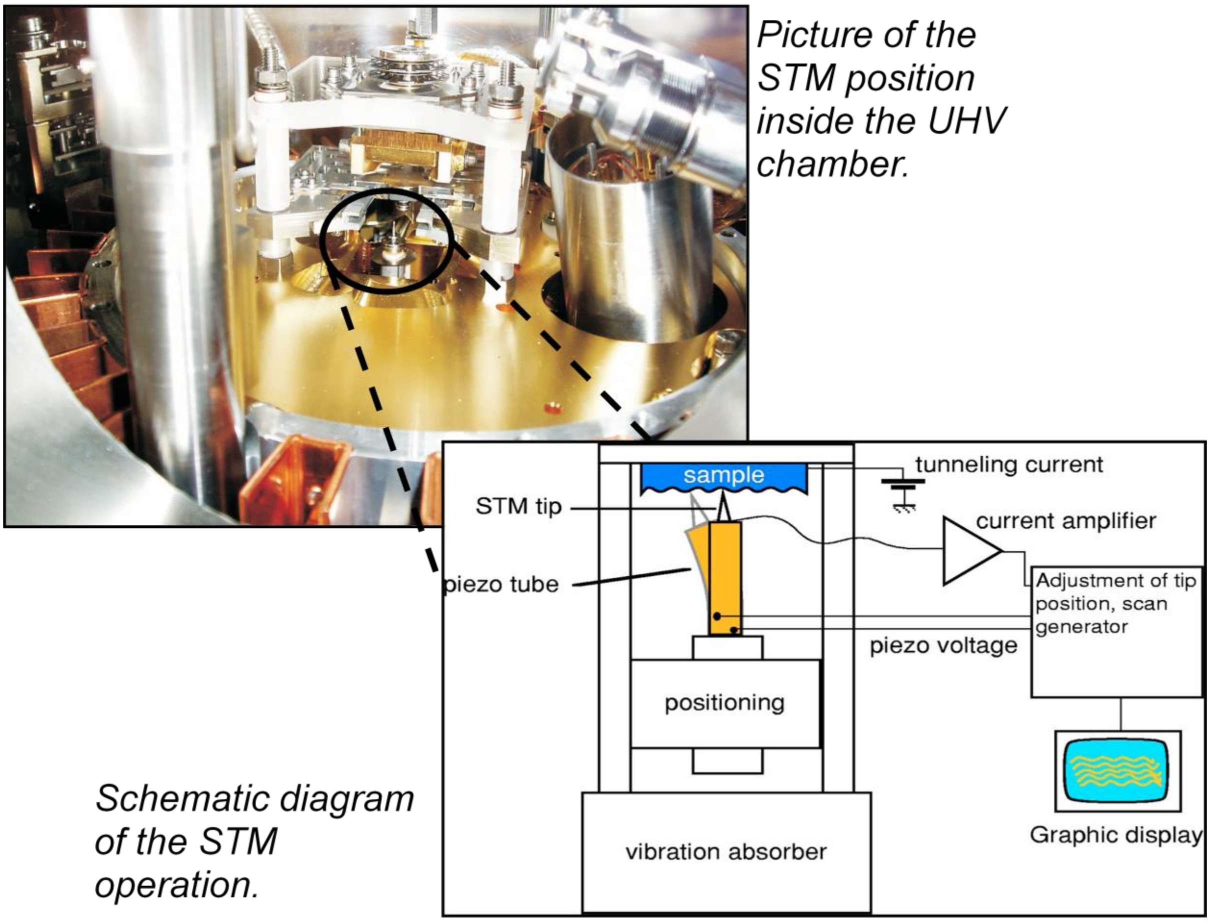

Figure 11 Photographic and schematic diagram of the STM [9, 20]. The STM data collected was obtained by using an Omicron VT-STM.

2.4 Thin-Film Growth of Pb

The entire apparatus is split into the preparation and analysis chamber. Inside the preparation chamber the sample is sputtered and annealed. Once it is ready for study the sample can be transferred to the analysis chamber to begin its investigation with the required technique.

In this investigation the technique used for data acquisition was with STM. Initially a tungsten tip was used to scan the surface of the quasicrystal to find good terraces for the deposition of Pb. Thereafter, the initiation of the depositing of Pb from a Pb evaporator that is fixed onto the analysis chamber began. The Table below shows the number of depositions, the time period, flux of the depositions and coverages in units of monolayers:

Number of Deposition	Time (min)	Flux (nA)	Coverage (ML)
1	5	120	1.2
2	5	120	2.4
3	5	240	4.8
4	5	240	7.2
5	5	240	9.6
6	5	240	12
7	5	240	16.8
8	5	240	31.2

Table 2 Table showing the amount of coverage on the quasicrystal substrate.

An atomically resolved image of the clean surface of the quasicrystal is shown here:

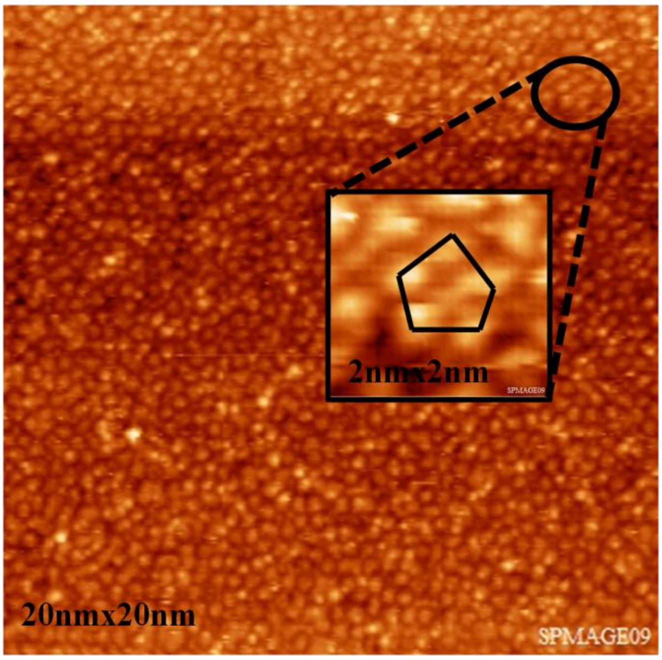

Figure 12 STM image of the Clean Surface.

The first two depositions show no evidence of Pb islands however the Pb atoms illustrate strong correlations with the structure of the quasicrystal.

The image below shows an atomic overlayer of Pb that has the quasicrystalline structure. The 10 atoms in the circle are the edge of a fivefold symmetry being rotated around the circle.

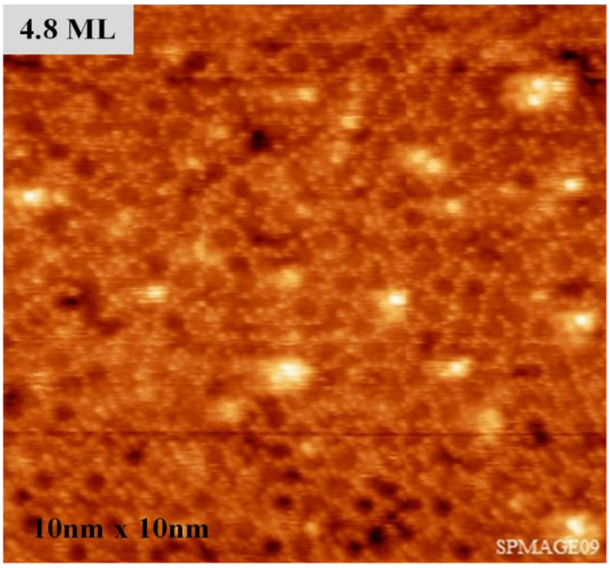

Figure 13 STM image of 4.8 ML of deposited Pb.

With increasing coverage of Pb the islands become noticeable from the 4.8 ML. The STM images below show the distribution of the islands for coverages varying from 4.8 ML to 31.2 ML:

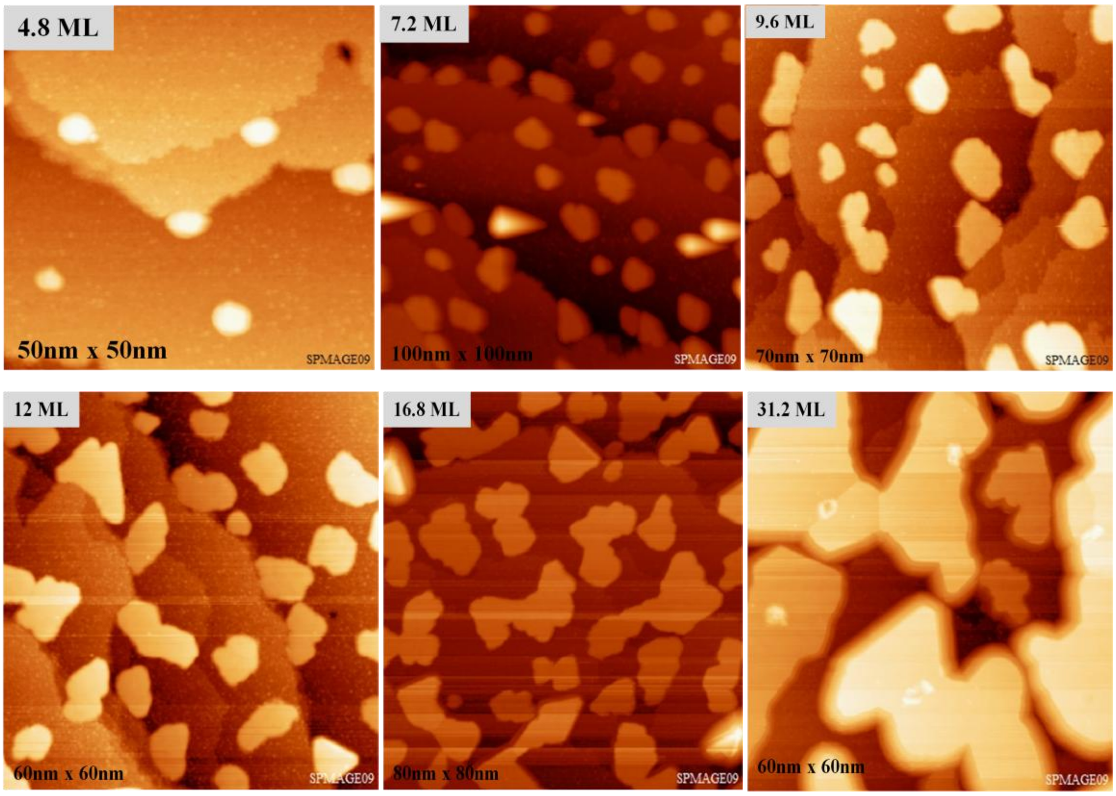

Figure 14 STM images with islands for each coverage collected.

The shapes of islands fall in the *compact island* category. This category is classified as islands that are square, rectangle, triangle or hexagonal shape with reasonably straight and equiaxial edges. The other classification of islands fall under the *ramified islands* and these are usually rough island edges, and dendrite structures [13].

At high coverages the islands appear to coalesced, i.e. they tend to merge upon direct contact and form into one island. However, the majority of islands do not coalesce due to the fact that Pb(111) forms an hexagonal close packed structure. Furthermore, the angle difference between islands due to rotational epitaxy prohibits them to merging into one single island.

Chapter 3

Data analysis

3.1 Data Analysis

The heights of each island from the STM images were measured using WSxM software in the following way:

1) An image with clear and visible islands was chosen. Blurred islands were not measured.
2) The *local plane* of the entire image was taken. This was done by choosing an area where the terrace is flat. This process levels out the base of the islands so that it is constant through the image.
3) A particular island was selected by zooming into it. The *profile line* application was used for all islands. With this application a line can be created that is put across the island. In turn this produces a graph that depicts the height and width of the island.
4) The profile line was done both in the vertical and horizontal direction.
5) Measurements of the *histogram height* of the islands were also taken. This application reads all of the heights present in the zoomed image and outputs a histogram graph that displays usually two peak heights. By placing the cursor on each peak one is able to read the height of that particular island. The first peak represents the most frequent height found at the flat area around the island. The second peak represents the most frequent height found at the top island.
6) This procedure is conducted for every single island in the STM image and done for all the images in each deposition. However, images with repeated islands on the same terrace were not recorded.

For the purpose of data analysis, only the values of the histogram heights are being taken into account. The vertical and horizontal heights were employed for the purpose of height consistency, however, the histogram height give the most accurate value as it reduces systematic errors that can occur when measuring the heights manually (e.g. when reading the height of an island with profile line, one places the cursor on a certain height, but from the profile graph one can see that the height oscillates throughout the graph.

3.2 Results

The data were plotted on histogram graphs to give an outlook of the most frequent heights. These histogram graphs shown below are for each coverage carried during the experiment:

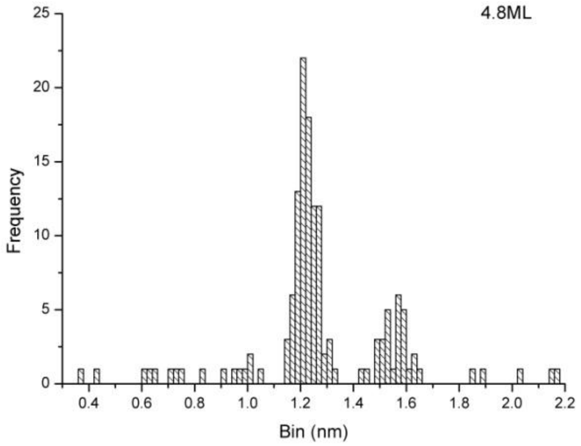

Figure 15 Histogram graph of 4.8 ML coverage.

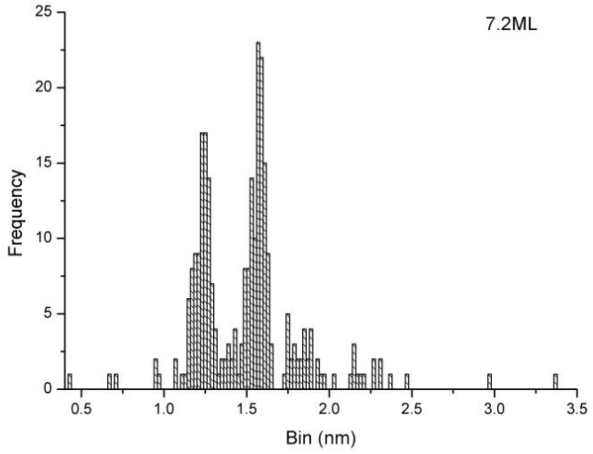

Figure 16 Histogram graph of 7.2 ML coverage.

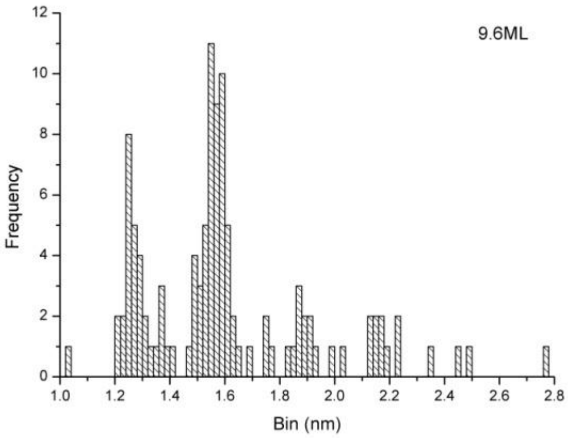

Figure 17 Histogram graph of 9.6 ML coverage.

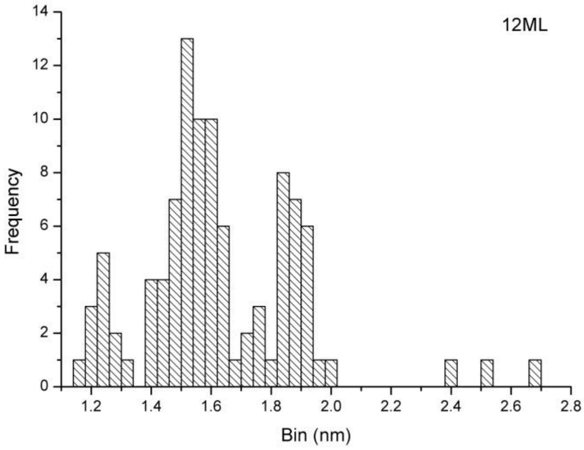

Figure 18 Histogram graph of 12 ML coverage.

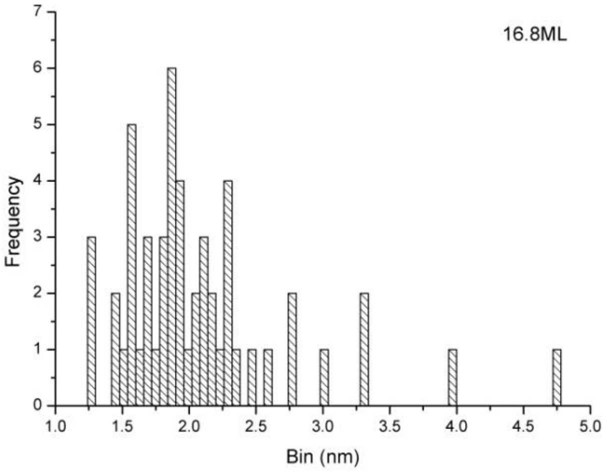

Figure 19 Histogram graph of 16.8 ML coverage.

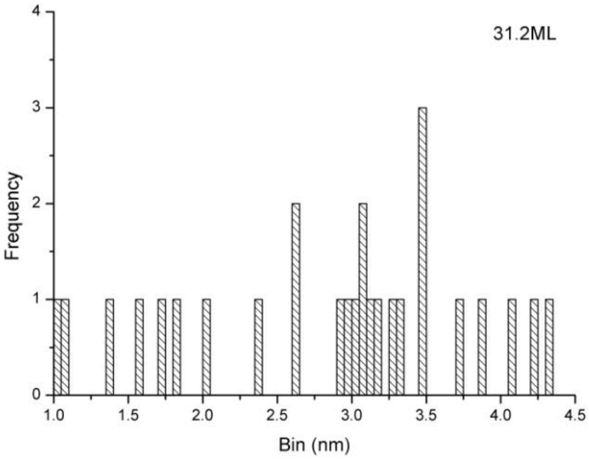

Figure 20 Histogram graph of 31.2 ML coverage.

It was noticed that certain heights dominated more than others. From these graphs it was possible to see that the most frequent heights would be around the heights of 1.2 nm, 1.5 nm and 1.8 nm.

The Table below shows the most frequent heights and its occurrence for each coverage:

Coverage (ML)	Number of Islands for the Selective Heights		
	1.2 nm	1.5 nm	1.8 nm
4.8	66	20	2
7.2	64	77	14
9.6	21	38	7
12	9	27	15
16.8	3	6	9
31.2	0	1	1

Table 3 Table showing the most frequent heights observed and its corresponding occurrences in relation to the coverage.

Below is a graph showing the number of islands versus its corresponding coverage for the selective heights.

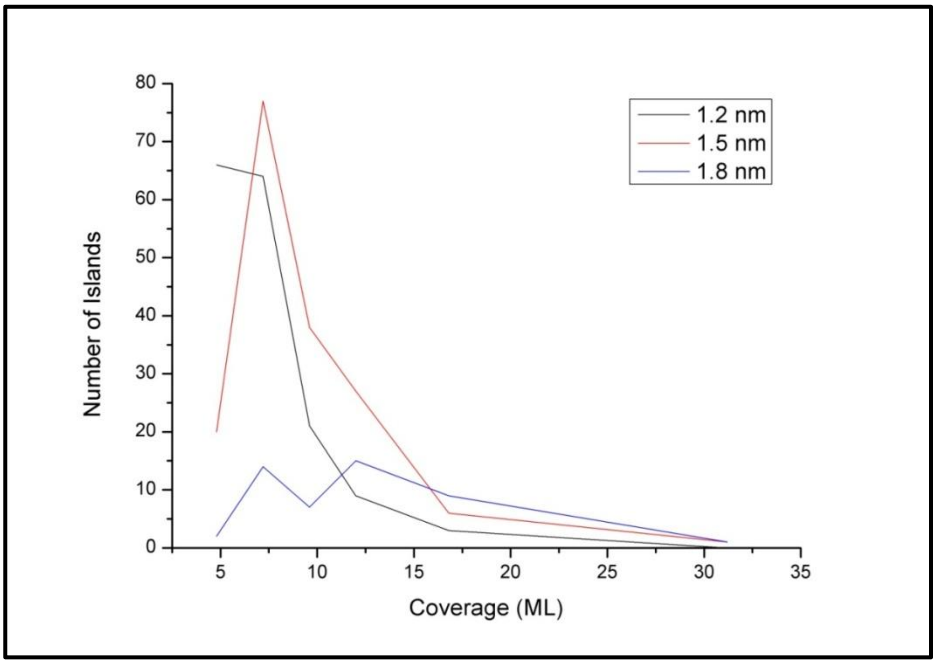

Figure 21 Graph of Number of Islands vs Coverage.

An average over all coverage was found for the selective heights and for some heights that seem to be dominating at the higher coverages. The Table below shows the outcome value for these frequent heights:

Selective Height (nm)	Average value across all coverages[4]	Monolayer (ML)
1.2	1.24 ± 0.026	4.3
1.5	1.56 ± 0.027	5.5
1.8	1.86 ± 0.027	6.5
2.4	2.46 ± 0.028	8.6
3.3	3.33 ± 0.031	11.6

Table 4 Table showing the average outcome values for frequent heights.

The value of the island heights in Monolayers was calculated by dividing the average height by the Pb(111) bulk interplanar distance (d_{Bulk} = 2.86Å):

$$Monolayers\ (ML) = \frac{Average\ Height}{d_{Bulk}} \tag{9}$$

The Monolayers heights observed in this experiment will be compared and discussed in the next section (See Discussion, Chapter 4). The values from **Table 4** will be compared with the values from **Table 5** which is a combination of height values (in units of Monolayer and nanometers) observed from previous experiments carried with Pb on different substrates.

---

[4] The average values and errors were obtain with OriginPro programme. The error is the standard deviation of the average value.

Chapter 4

Discussion and Conclusion

4.1 Discussion

This studied system of Pb on Ag quasicrystal showed to have certain heights that could possibly be the evidence of “Magic Heights”. The most occurring heights on the entire system were 1.24nm, 1.56nm and 1.86nm. From **Figure 21** one notices that the number of 1.2 nm island heights decrease. This is due to the fact that with increase coverage the 1.2 nm islands become damped out while the 1.5 nm and 1.8 nm continue to increase. However at 9.6ML the 1.5 nm islands are damped while the 1.8 nm islands continue to oscillate in the number of islands. There is a drop for the 1.8 nm islands from 16.8 ML to 31.2 ML due to the fact that there were not enough suitable islands to carry a good statistical evaluation on the number of islands.

A monolayer value for each selective height was obtained by dividing the island heights with the value of the Pb(111) bulk interlayer separation (d_{Bulk} = 2.86Å). The acquire values from this experiment can be compared with other experiments in which Pb was deposited on other single metal substrate.

Otero *et al* conducted an experiment in which Pb was deposited on Cu(111) at 300 K and above [21]. The growth mode on this experiment was reported to be Stranski-Krastanov, which is also the growth mode for the system studied in this experiment. It also stated that its island heights where an integer number of the Pb(111) interplanar distances (2.86Å). In addition, it was affirmed that certain height were more frequent than other. Its “Magic Heights” or the allowed heights were the 6, 8, 10, 11, 15, 17, and 20 ML islands and the 5, 9, 12, 14, 18, 19, and 21 were the “forbidden” heights or the heights that appeared less frequently. By conducting local spectroscopy characterization it was noticed that the allowed heights were those that would have their QWS’s far from the Fermi Level and the “forbidden” heights were those that had their QWS’s close to the Fermi Level.

The observed island heights in this report do not show any direct relation to the numbers stated in [21]. Due to the fact that there is not much data at higher coverages, it is difficult to compare the results with the “forbidden” and allowed heights. The obtained results in this report appear to be oscillating around the “forbidden” and allowed heights. This oscillation can be explained by another experiment conducted.

In an experiment carried by Crottini *et al* [22] it was noticed that when Pb was deposited on Ge(111) the islands height demonstrated to have an oscillation of ±15% around the bulk Pb(111) interplanar distance but it gradually was dampened out after the deposition of a dozen monolayers. This oscillation behaviour on Crottini *et al* experiment was observed earlier by Feibelman where quantum size fluctuations were observed for thin films of Al(111) and Mg(0001). It was noticed that the electron density and work function were related to the relaxation of the outermost interplanar distance so that the total energy could be minimised [23].

Such oscillations would be more favoured in the system being reported in this project. **Table 5** is a combination of the theory between Otero and Crottini. The table shows that it if the theory of oscillation is applied to the theory of “allowed” heights then the values of island heights for Pb/Ag-In-Yb are allowed heights due to the fact that relaxation could be occurring in these islands.

In another investigation by Hupalo and Tringides, it was observed that islands heights of Pb on Si(111) also showed differences between preferred and not preferred island heights. The islands were grown at low temperatures and the preferred heights differed by bilayer height increments ($2d_{bulk}$ is the single-step height for Pb(111)) [24] The most stable heights had values of: 5.2, 7.2, and 9.2 ML while the unstable heights had values of 6.3 and 4.2 ML. These values are also within the oscillations observed in **Table 5** however they do not correlate with the values obtained in this experiment.

As mentioned earlier the value of the island heights in this studied system could show evidence of “Magic Heights” because it was observed in a previous experiment [5] that when Bi is deposited on top of a quasicrystal substrate it showed that certain heights were more dominant than others.

However, it is not possible to prove that the heights obtained are the “Magic Heights” of this system without having observed quantum size effects (See Recommendation Section on how to observe quantum size effects).

The explanation of these selective heights arises from the fact that the quantum well states (QWS) and the total electronic energy are depended on the film height. If the contribution to the electronic energy to the total energy is significant, then some sizes will be energetically more favoured than others [21]. Furthermore, the most stable film thicknesses are those which have the QWS far below the Fermi Level. This is due to the fact that electrons prefer to be at much lower levels than at higher ones as it would require much energy to stay in such levels.

The Table below showing a combination of the values observed from Otero *et al* and Crottini *et al*. The allowed layers are results from Otero et al. The experimental height is obtained by dividing the allowed layers with d_{Bulk} to find its height in terms of nanometres. The experimental height is then subtracted and added by 15% to have an overview of the possible oscillations that these “Allowed Layers” could have if they obeyed quantum fluctuations. Its Monolayers are also stated:

Allowed Layer (ML)	Experimental Height (nm)	Height – 15%	Monolayer (ML)	Height + 15%	Monolayer (ML)
6	1.716	1.459	5.1	1.973	6.9
8	2.288	1.945	6.8	2.631	9.2
10	2.86	2.431	8.5	3.289	11.5
11	3.146	2.674	9.4	3.618	12.7
15	4.29	3.646	12.8	4.934	17.3
17	4.862	4.133	14.5	5.591	19.5
20	5.72	4.862	17	6.578	23

Table 5 Table showing the “allowed” heights with theoretical values of quantum-size oscillation.

4.2 Conclusion

In conclusion, it is feasible to say that there are certain islands heights of Pb on Ag quasicrystal substrate that are strongly preferred compared to others. The 1.24 nm, 1.56 nm and 1.8 nm showed great dominance throughout the early coverages. The 2.46 nm and 3.33 nm showed themselves to be more frequent, however, there was not enough data with islands at these coverages that could confirm this. The energy impact of the QWS has a great influence in the stability of islands. It determines on the equilibrium size of the nanoislands. The quantum size effects that are a result of the confinement of the electrons are manifested by the electronic structure of the quasicrystalline substrate.

Although the obtain heights in this report were not precisely consistent with experiments carried out with similar procedure, it is possible to hypothesis that the Pb islands might be expanding or relaxing around its stable heights. Exact prove is required to establish if these heights are the selective heights, therefore, techniques that will probe the energy of the outermost electrons can provide with information that is needed for a greater understanding of this system.

4.3 Outlook

There are several ways of carrying an investigation forwards. One of the most important aspects of experiments is to be able to reproduce your data. Thus one suggestion for the continuation of this project is to repeat the experiment and see if the data is reproducible.

Producing large scale STM images can ensure that they show a statistical significant part of the film, while still allowing a clear identification of the island heights.

To observe the quantum size effects (QSE), it is recommended to use Ultraviolet Photoelectron Spectroscopy (UPS) [16]. This technique can probe the outer electrons or valence electrons.

Electron Spectroscopy uses the energy of photons to excite electrons. The kinetic energy of the ejected photoelectrons is measured using an electro-static analyser [18]. Usually, Electron Spectroscopy operates under UHV conditions so as to increase the mean free path of ejected electrons.

Ultraviolet light can be obtained from certain light sources such as Helium I, Helium II and Ne I. These light sources radiate low energy photons in the order of 10 – 40eV. Having low photon energy in UPS means that the deep core level electrons cannot be excited but it is sufficient for the valence electrons.

The photoemission of the various electron states can be used to determine the density of states. The existence of QSE can be determined by measuring the density of states near the Fermi level. The QWS close to the Fermi Level will enhance the density of states at the Fermi Level but as mentioned before, only the QWS well below the Fermi Level will give rise to an enhanced stability of the film thicknesses.

Another quantum mechanical tool to probe the quantum world is the Scanning Tunnelling Spectroscopy (STS). This technique is able to explore the local density of states and the band gap of substrate-film and film-vacuum interfaces. STS operate much like STM in which it can operate in the constant current mode or in the constant height mode to produce topographical images. The additional operation for this technique is that it is able to produce measurements of current versus voltage at the certain x, y position, i.e. it is a measurement of the tunnelling current with respect to the tip-sample bias.

4.4 Systematic and Random Errors

All measurements obtained in this investigation are prone to systematic and random errors. Errors occur when scanning is taking place. The resolution of the information being analysed can be decreased on the sharpness of the tips used and on the signal given out. Although the chances are minimal, there are possibilities of the sample and islands being contaminated by impurities in the surrounding environment of the UHV. When finding the island heights there is great chances that if the measurement is repeated, the outcome value is almost always different. There will certainly be unpredictable fluctuations in the readings of a measuring apparatus or programmes therefore the final values will never be the same.

Acknowledgements

I would like to thank Dr. Sharma for his supervision, Peter Nugent for his support in the experimental side, Joe Smerdon for his help in experimental and theoretical side and the rest of the group for their support.

Bibliography

[1] Tsai, A. P. et al. (2000). *Nature, 408*, 537.

[2] Sharma, H. R., Shaimoda, M. and Tsai, A. P. (2007). Quasicrystal surfaces: Structure and growth of atomic overlayers. *Taylor & Francis, 56*(3-4), 403-464.

[3] Dubois, J., Kang, S. S., & Perrot, A. (1994). Towards applications of quasicrystals. *Materials Science and Engineering A, 179-180*(Part 1), 122-126.

[4] Sharma, H. R. *Second Layer of Pb on i-Ag-In-Yb.* Surface Science Research Centre (Personal Communication)

[5] Sharma, H. R., et al. (2008). Growth of bi thin films on quasicrystals surfaces. *Physical Review B, 78*(155416), 1-9.

[6] Janot, C. (1992). 1. how to fill space with atoms in condensed matter states. *Quasicrystal A primer* (Second edition ed., pp. 1-2). United States: Oxford University Press.

[7] Lucas, C. (2006). *Condensed matter physics.* Unpublished manuscript.

[8] Shechtman, D., Blech, I., Gratias, D. and Cahn, J. W. (1984). **Metallic phase with long-range orientational order and no translational symmetry**. *Physcal Review Letters, 53*(20), 1951-1953.

[9] Smerdon, J. (2006). The formation and characterisation of aperiodic ultra-thin films on the surface of quasicristals. Department of Physics, University of Liverpool).

[10] Bourne, M. (2008). *The math behind the beauty*. Retrieved April, 2009, from http://images.google.co.uk/imgres?imgurl=http://www.intmath.com/Numbers/beautyMath/body_sm_ratios.jpg&imgrefurl=http://www.intmath.com/Numbers/mathOfBeauty.php&usg=__C26-fwW0fZ8jA8rfhsD19V11vBg=&h=314&w=300&sz=10&hl=en&start=39&um=1&tbnid=oY-dvV_bJcxHJM:&tbnh=117&tbnw=112&prev=/images%3Fq%3Dgolden%2Bration%26ndsp%3D18%26hl%3Den%26client%3Dfirefox-a%26rls%3Dorg.mozilla:en-GB:official%26sa%3DN%26start%3D36%26um%3D1

[11] Unknown. *Icosahedron.* Retrieved April, 2009, from http://en.wikipedia.org/wiki/File:Icosahedron.svg

[12] Prutton, M. (1998). 3. surface structure - scanning tunnelling microscopy (STM). *Introduction to surface physics* (Third ed., pp. 90-95). New York: Oxford University Press.

[13] Oura, K. e. a. (2003). 14. growth of thin films. *Surface science an introduction* (pp. 357-358-386). Germany: Springer-Verlag Berlin Heidelberg.

[14] McGrath, R. (2009). *Nanoscale physics and technology.* Unpublished manuscript.

[15] Chiang, T. C. (2000). Photoemission studies of quantum well states in thin films. *Surface Science Reports, 39*, 181-235.

[16] Milun, M., Pervan, P. and Woodruff, D.P. (2002). Quantum well structures in thin metal films: Simple model physics in reality? *Reports on Progress in Physics, 65*, 99-101-115.

[17] IBM. *Scanning tunnelling microscopy*. Retrieved April, 2009, from http://www.almaden.ibm.com/vis/stm/

[18] Sharma, H. R. (2009). *Surface physics.* Unpublished manuscript.

[19] Nugent, P. *Tip creation*. Surface Science Research Centre.

[20] Hofer, W. A., Foster, A. S. and Shluger, A. L. (2003). Theories of scanning probe microscopes at the atomic scale. *Reviews of Modern Physics, 75*, 1288-1289.

[21] Otero, R., Vazquez de Parga, A. L. and Miranda, R. (2002). Observation of preferred heights in pb nanoislands: A quantum size effect. *Physical Review B, 66*(115401), 1-5.

[22] Crottini, A., Cvetko, D., Floreano, L., Gotter, R., Morgante, A. and Tommasini, F. (1997). Step height oscillations during layer-by-layer growth of pb on ge(001). *Physcal Review Letters*, *79*(8), 1527-1529.

[23] Feibelman, P. J. (1983). Static quantum-size effects in thin crystalline, simple-metal films. *Physical Review B, 27*(4), 1991-1996.

[24] Hupalo, M. and Tringides, M. C. (2002). Correlation between height selection and electronic structures of the uniform height Pb/Si(111) islands. *Physical Review B, 65*, 115406.

[25] Dil, J. H. and Kim, J. W. (2004). Self-organization of pb thin films on cu(111) induced by quantum size effects. *Physical Review B*, *70*, 045405.

[26] Kawakami, R. K., Rotenberg, E., Choi, H. J., Escorcia-Aparicio, E. J., Bowen, M. O., Wolfe, J. H., et al. (1999). Quantum-well states in copper thin films. *Letters to Nature, 398,* April 2008-132-134.

[27] Ossi, P. M. (1953). 6. quasicrystals. *Disordered materials - an introduction* (pp. 231). Germany: Springer.

[28] Sharma, H. R. (2009). *Quasicrystal surfaces.* Unpublished manuscript.

[29] Venables, J. A. (2000). 3.3 inelastic scatering techniques: Chemical and electronic state information. *Introduction to surface and thin film processes* (pp. 76-87). United Kingdom: Press Syndicate of the University of Cambridge.

Glossary of Acronyms

STM – Scanning Tunnelling Microscopy

UHV – Ultra High Vacuum

VT – Variable Temperature

Pb – Lead

List of Figures

List of Tables